Interaction of the Chlorine Atom with Water: ESR and ab Initio MO Evidence for Three-Electron ($\sigma^2\sigma^{*1}$) Bonding

Michael D. Sevilla,*,† Steven Summerfield,† Isaac Eliezer,† Janusz Rak,† and M. C. R. Symons‡

Department of Chemistry, Oakland University, Rochester, Michigan 48309, and School of Applied Sciences, De Montfort University, Leicester, U.K.

Received: December 16, 1996; In Final Form: February 11, 1997[⊗]

The specific interaction of chlorine atoms with water has been investigated by electron spin resonance spectroscopy and molecular orbital theory. Chlorine atoms are formed by attack of hydroxyl radicals on chloride ions in frozen aqueous solutions at low temperatures. A variety of frozen aqueous systems were irradiated at 77 K and investigated by ESR spectroscopy, and results obtained suggest a localized three-electron bond ($\sigma^2\sigma^{*1}$) between •Cl and H_2O or less likely with OH^-. Chlorine atom interactions with both species were investigated by both ab initio and semiempirical molecular orbital calculations. A series of isolated chlorine−water radical species consisting of hydrated chlorine atoms as well as chloride anions with hydroxyl radicals were considered. Best agreement with experiment is found for chlorine atom−water interactions, $H_2O-\dot{C}l(H_2O)_n$. Full optimization of •OH−Cl^- aquated systems shows that energetic ion dipole forces overcome weaker $\sigma\sigma^*$ interactions and result in full spin localization on the hydroxyl radical. Poor agreement with experiment is found even when the Cl•OH^- structure is held in position to promote $\sigma\sigma^*$ bonding. However, for $H_2O-\dot{C}l(H_2O)_n$ ($n = 0$, 2 and 5 considered) a comparison of the experimental hyperfine couplings and spin densities suggested from experiment, i.e., 60% spin on the chlorine atom, with the results found from ab initio calculations, gives improved agreement as n increases, with best agreement found for $n = 5$. The theoretical results support the formation of a water−chlorine three-electron bond with a substantial sharing of the unpaired spin between the bonding entities.

Introduction

The interaction of chlorine atoms with water has been a topic of continuing interest.[1−5] Any bonding interactions will have important implications for the reactivity of this species in aqueous solution. In work on the flash photolysis of $•Cl_2^-$ and other radicals,[1] Nagarajan and Fessenden concluded that photolysis of aqueous chlorine atoms resulted in the hydroxyl radical and chloride ion (reaction 1). This reaction was considered to be direct evidence for a charge-transfer absorption band involving chlorine atoms and water solvent that had been originally proposed in earlier work by Treinin and Hayon.[3,4]

$$•Cl(H_2O)_{(aq)} \xrightarrow{h\nu} Cl^-_{(aq)} + OH•_{(aq)} + H^+_{(aq)} \qquad (1)$$

Jayson, Parsons, and Swallow, in their pulse radiolytic work on chloride ion in aqueous solution,[2] described the reaction of the hydroxyl radical with chloride ion as having steps shown in reactions 2−4. The overall equilibria shown in reactions 2 and 3 favor the reactants at neutral pH:

$$Cl^-_{(aq)} + OH•_{(aq)} = •ClOH^-_{(aq)} \quad K_{eq} = 0.7 \qquad (2)$$

$$H^+_{(aq)} + •ClOH^-_{(aq)} = Cl•_{(aq)} + H_2O_{(aq)} \quad K_{eq} = 1.6 \times 10^7 \qquad (3)$$

$$•Cl_{(aq)} + Cl^-_{(aq)} = •Cl_2^-_{(aq)} \quad K_{eq} = 1.9 \times 10^5 \qquad (4)$$

The intermediate •$ClOH^-$ (or possibly •$Cl(H_2O)$) was described in these experiments (see also Hayon and Treinin[3,4]) as having an absorbance band with $\lambda_{max} = 320$ nm and $\epsilon_{340} = 3800$ M^{-1} cm^{-1}. However, recently, Adams et al. find[5] no absorption at all for chlorine atoms at these wavelengths and, consequently, find the equilibrium constant for reaction 4 to be $(4.7 \pm 0.4) \times 10^3$ dm^3 mol^{-1}, i.e., 40 times smaller than the originally reported[2] value of 1.9×10^5 dm^3 mol^{-1}.

The reaction of the hydroxyl radical with the chloride ion (reaction 2) is intriguing. The hydroxyl radical electron affinity is 1.83 eV,[6] and the ionization potential of the chloride ion is 3.61 eV.[7] As a consequence, a charge transfer in the gas phase is unfavorable by nearly 1.8 eV; however, in solution, this transfer may become more favorable thermodynamically owing to the solvation energies of product species. In solution any bonding between the OH radical and Cl^- would depend on the stabilization of the charge-transfer intermediate. The interaction of water and the chlorine atom appears plausible in the gas phase. Water has an ionization potential of 12.6 eV and that of the Cl atom is 13.0 eV, which implies the water HOMO is close to that of the Cl atom SOMO, and this creates the potential for a $\sigma^2\sigma^{*1}$ ($\sigma\sigma^*$ for brevity) bonding interaction.[7−16] This type of bonding occurs when a radical with localized spin interacts with a lone pair on another molecule to produce a localized three-electron bond.[13] The σ^* orbital in $\sigma\sigma^*$ bonding contains the unpaired electron, which is largely confined to the two bonding atoms with little delocalization into the remainder of the molecular structure. In Table 1 a number of examples of this type of bonding are provided. A good example of this type of bonding is that found for the interaction of a Cl atom with the nitrogen lone pair in pyridine in which 98% of the unpaired spin is localized to the two bonding atoms, 55% on Cl and 43% on N.[9]

In this study, we present the first evidence for a three-electron-bonded chlorine atom−water species. This evidence comes from experimental electron spin resonance studies on irradiated aqueous solutions of chloride ion at low temperatures and is in

† Oakland University.
‡ De Montfort University.
⊗ Abstract published in *Advance ACS Abstracts,* April 1, 1997.

S1089-5639(96)04097-2 CCC: $14.00

TABLE 1: Hyperfine Parameters for Chlorine Atoms $\sigma\sigma^*$ Bonded to Various Heteroatoms (X)

Cl−Ẋ	$A_{\|}(^{35}Cl)/A_{\|}(X)$ (G)	$A_{\perp}(^{35}Cl)/A_{\perp}(X)$ (G)	$g_{\|}/g_{\perp}$	$\rho(^{35}Cl)^a/\rho(X)$	ref
Cl−Ċl$^-$	101	(10)	2.00/2.038	0.50	8, 9,13
Cl−ȮH$^-$($SrCl_2$)	59	(16)	2.00/2.017	0.29	12
Cl−Ȯ$H_{2(aq)}$	122	(20)	2.01/2.06,2.04	0.60	this work
Cl−ṄH_3					
(^{35}Cl)	43.3	13.5		0.21	10
(^{14}N)	46.5	9.0		0.74	
Cl−ṖMe_3					
(^{35}Cl)	75	40	2.00/2.01	0.37	8
(^{31}P)	730	560		0.55	
					
(^{35}Cl)	112	22		0.55	9
(^{14}N)	66	42		0.43	
					
(^{35}Cl)	115	24	2.00/2.028	0.56	11
(^{14}N)	68	45		0.45	
Cl−Ṡ(R)(CH_3)	71	<15		0.35	13

[a] Calculated using $\rho(X_{exp}) = B(X_{exp})/B(\rho = 1)$ with $B(\rho = 1) = 17$ G for N-14, $B(\rho = 1) = 102.4$ G for P-31, and $B(\text{exp}) = [A_{\|} - A_{\perp}]/3$. $\rho(Cl_{exp}) = A_{\|}(Cl_{exp})/202$ G.

agreement with ab initio and semiempirical molecular orbital calculations performed in this work.

Experimental Section

All chemicals were commercially available reagent grades and were used without further purification. Aqueous solutions containing chloride salts and various other solutes were prepared in N_2-bubbled H_2O or D_2O drawn into quartz tubes and frozen in liquid nitrogen (77 K). All samples, unless otherwise stated, were γ-irradiated to 1.0 Mrad at 77 K. A Varian Century spectrometer operating at 9.3 GHz with an E-4531 dual cavity, 9 in. magnet, and low-temperature accessory was employed to record ESR spectra. Fremy's salt was used as a comparison standard for hyperfine couplings and g values (A_N =13.09 G, g = 2.0056). The other experimental conditions were detailed elsewhere.[13]

The computational results presented in this paper were performed at both semiempirical and ab initio levels of theory. All calculations were carried out using GAUSSIAN 94[17] and SPARTAN (Wavefunction, Inc., Irvine, CA) program packages. Since the paper is devoted to the description of open-shell systems, the unrestricted (UHF) approach was used at both semiempirical and ab initio levels. Spin contamination was found to be small, with typical expectation values of $\langle S^2 \rangle$ of 0.75−0.77, which justifies the choice of the methodology. The semiempirical PM3 approach was employed for comparison to ab initio results and to extend calculations to larger systems.[18] Ab initio calculations were carried out with the split valence 6-31G* or 6-31+G* basis sets.[17,19,20] Calculations with diffuse functions (6-31+G*) were found to improve the description of anionic species. Ab initio calculations were performed at the unrestricted Hartree−Fock[21,22] level with correlation corrections made at the MP2[23] level using the frozen core approximation.[17] For comparison purposes a DFT computation was performed with a local spin-density approximation[24] using local Slater[25] exchange and Vosko, Wilk, and Nusair[26] correlation functionals (LSDA/SVWN). The basis set used was DN**, which roughly corresponds to a 6-31G** basis set. Constrained or unconstrained gradient geometry optimizations[27] were carried out to obtain structure and properties of systems under consideration. Mulliken population analysis[28] on SCF densities was performed to find required spin and charge distributions. Such calculations have given acceptable results in similar systems.[13,29,30] All computations were performed on Silicon Graphics Indigo2 and Cray-YMP computers.

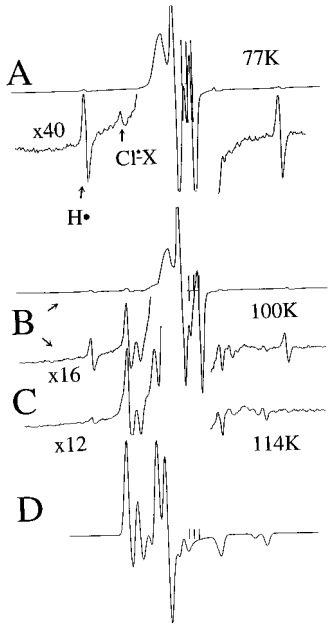

Figure 1. First derivative ESR spectra of a frozen aqueous solution of 0.02 M NaCl after γ-irradiation at 77 K (A) and annealing (B, C). The stepwise development of the ESR signal of the Cl−Ẋ species is observed on annealing. Part D shows a computer simulation of the anisotropic spectrum of the Cl−Ẋ species using **g** and hyperfine tensors described in the text. The three markers in the center of the spectra in parts A, B, and D are separated by 13.09 G with the center component at g = 2.0056. The hydrogen atom resonances in parts A and B are separated by 506 G.

Results and Discussion

ESR Results. After γ-irradiation of a variety of frozen aqueous solutions dilute in Cl^-, we have observed a monochlorine species having a $A_{\|}$ Cl-35 coupling of ca. 122 G and a $A_{\|}$ Cl-37 coupling of 102 G. We find the same couplings in frozen aqueous solutions of sodium chloride alone (0.02 M; see Figure 1) or NaCl in 3 M H_3PO_4 (Figure 2). In addition, dilute Cl^- in frozen aqueous solutions of a variety of solutes at 0.3−3 M concentrations, i.e., $NaClO_4$, Na_2SO_4, H_3BO_3, $NaNO_3$, H_2SO_4, KH_2PO_4, and methanol, also gave similar spectra. In Figure 1

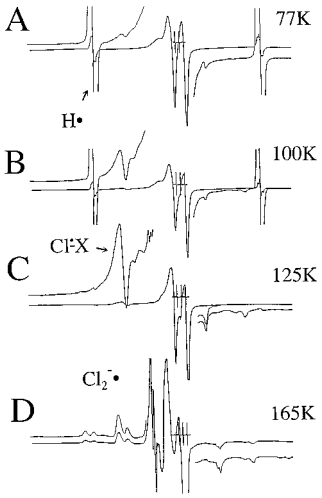

Figure 2. (A) ESR spectrum found after γ-irradiation at 77 K of a 3 M H_3PO_4 solution containing 0.02 M NaCl. (B, C) Spectra found on stepwise annealing to temperatures shown in the figure, which show the progressive increase in the Cl−Ẋ species. (D) On annealing to 165 K the spectrum of $^{\bullet}Cl_2^-$ is observed as the signal of the Cl−Ẋ species is lost. The three markers in the center of each spectrum are separated by 13.09 G with the center component at $g = 2.0056$.

we show the stepwise development of the signal of the $^{\bullet}$Cl−X species in an irradiated glassy 0.02 M NaCl solution. Parts A−C of Figure 1 show the gradual decrease in the hydroxyl radical signals and a corresponding increase in the spectrum of the $^{\bullet}$Cl−X species on annealing from 77 to 114 K. The species is uniquely identified by the ^{35}Cl and ^{37}Cl features both for their relative intensities, which are about 3:1, and for the relative hyperfine splitting constants, which show the expected ratio of Cl-37 to Cl-35 (1.20). An anisotropic computer simulation based on a Cl−Ẋ species with **g** tensor [2.06, 2.04, 2.01] and hyperfine tensors (in Gauss) of **A**(Cl35) [20, 20,122] and **A**(Cl37) [17,17,102] with a 12 G line width is shown in Figure 1D. This simulation is in good agreement with the outer components of experimental spectrum in parts A−C of Figure 1. However, the inner components are overlapped by the strong signal of the hydroxyl radical. Furthermore, some components of $^{\bullet}Cl_2^-$ are observed between those of Cl−Ẋ in the experimental spectrum. In Figure 2, we show the results of irradiation of a 3 M H_3PO_4 solution containing 0.02 M NaCl. Again, the amount of $^{\bullet}$Cl−X increases as the sample is annealed from 77 to 125K. The central doublet is due to both the phosphate and OH radicals. The line width of the $^{\bullet}$Cl−X species is broadened in this matrix, but the hyperfine coupling remains the same. On annealing to 165 K only the spectrum of the $^{\bullet}Cl_2^-$ radical is found (Figure 2D), which is likely a result of $^{\bullet}$Cl−X attack on Cl^-. Qualitatively, $A_\perp$ is much smaller than $A_{||}$ and $g_\perp$ is greater than $g_{||}$, which is in agreement with expectation for a $\sigma\sigma^*$-bonded Cl atom. These results suggest that the monochlorine species forms a single bond to a group, X, with an available electron pair and a nonmagnetic nucleus. Since the parameters are invariant for different frozen aqueous solutions including the 0.02 M NaCl solution, it would appear that X is H_2O or OH^-. The features narrow using D_2O media, as expected.

The results found in this work and those for related $\sigma\sigma^*$ radicals[8−13] where Cl^- is one component are given in Table 1. For Cl_2^-, the parallel chlorine hyperfine coupling [$A_{||}$(Cl-35)] is 101 G (see Table 1).[8,9] Assuming that for $Cl_2^{\bullet-}$ the spin density on each atom is 50% and assuming that $A_{||}$ is approximately proportional to the spin density, we estimate the spin density on each Cl atom in Table 1 from the following simple relationship: ρ(Cl-35 = $A_{||}$(Cl-35)/202. In cases for which $A_\perp$ is known, the values for the 3p-orbital population, calculated in the usual way from the isotropic and anisotropic components, agree quite well with estimates from this relationship. Other than $Cl_2^{\bullet-}$, the best defined centers are those with Cl−N σ^* bonds,[9−11] since they give well-defined coupling to ^{14}N. In these cases the total calculated spin densities are quite close to unity as expected for localized $\sigma\sigma^*$ bonding.

Since the $^{\bullet}$Cl−X species is formed by direct radiation damage at 77 K and by $OH^{\bullet}$ attack on chlorine on annealing, it might be assumed that the intermediate formed is Cl−ȮH^-. However, for Cl−ȮH^- centers formed in irradiated $SrCl_2$,[12] $A_{||}$ is 59 G (see Table 1), which implies a spin density of ca. 0.3 (59/202) on Cl. The spin density distribution, therefore, favors $^{\bullet}$OH. The magnitude of the reported ^{1}H perpendicular coupling, which is about 25 G, confirms the spin distribution.[12] For comparison, the measured splitting for OH in ice[14] is about 40 G, suggesting an approximate spin-density of 0.6 on oxygen, in reasonable accord with the estimate on Cl, i.e., (0.3 + 0.6 = 0.9).

For the Cl−Ẋ species we observe, the spin density is 0.6 on the chlorine. This suggests a Cl−Ẋ complex with a species X that has more electron-withdrawing power such as water. Clearly, for a Cl−ȮH_2 species the σ^* SOMO would change to favor chlorine as observed in this work. By the same argument, but by comparison with $H_2O^{\bullet+}$ ($a_H \approx 24$ G),[15] the maximum ^{1}H coupling is predicted to be ca. 8 G. This is within the line width of the observed spectra. We note that the two species under consideration differ by a proton as indicated by the reaction

$$\text{Cl}-\dot{\text{O}}\text{H}_{2(\text{aq})} = \text{Cl}-\dot{\text{O}}\text{H}^-_{(\text{aq})} + \text{H}^+_{(\text{aq})} \qquad (5)$$

This reaction is the reverse of reaction 3 ($1/K_3 = 6 \times 10^{-8}$), and at pH 7 comparable amounts of the two species are suggested. At acid pH's employed in our work in 3 M H_3PO_4, Cl−Ȯ$H_{2(aq)}$ should be the dominant species. To help distinguish between the above alternatives, we performed ab initio calculations on several hydrated monochlorine species.

MO Calculations. Two model systems were considered: group A consists of species that investigate the interaction of chloride ion and hydroxyl radical; group B consists of species that investigate the interaction of the chlorine atom with water. The results for these structures are given in Table 2, and several of the important structures are shown in Figures 3 and 4.

Group A. Optimized ab initio and PM3 calculations for species of the type $Cl^-\cdots{}^{\bullet}OH(H_2O)_n$ with $n = 0-6$ invariably gave fully optimized structures with the OH dipole directed at the chloride ion, i.e., $Cl^-\cdots HO^{\bullet}$ (see Figure 3C). The ion−dipole interaction is clearly a stronger interaction than any bonding between oxygen and chlorine. As a consequence, in fully optimized structures no spin transfer was found and the spin was fully localized on the $^{\bullet}$OH oxygen in all these structures. The nature of the overall interactions in the solid state would likely stabilize other orientations. For this reason, ab initio calculations were performed with the ClOH bond angle fixed to allow for bonding between the localized half-filled p orbital on the OH radical oxygen and a chlorine ion lone pair. A local optimization at the PM3 level gave a ClOH bond angle of 96.3°. At this same orientation, slight interaction is found at 6-31+G*; whereas, none is found at 6-31G*(see Table 2). The + functions are clearly needed for a complete description of anionic species, and the improved interaction is expected. Addition of one water forms Cl−Ȯ$H(H_2O)^-$, and optimization of this species at UMP2/6-31G* [6-31+G*] (with the ClOH bond angle again fixed at 96.3°) results in a prediction of $\sigma\sigma^*$ bonding with a 14% [27%] transfer of spin to chlorine and a Cl−O distance indicative of bonding (see Table 2 and Figure 3B). At 6-31+G* the calculated spin density on the hydroxyl

TABLE 2: MO Calculations on $\sigma\sigma^*$ Bonding in $Cl-OH(H_2O)_n^{\bullet-}$ and $^{\bullet}Cl(H_2O)_n$ Species

	PM3					MP2[a]					
	Cl−O (Å)	Cl charge	ρ_{Cl}	ρ_O	$\sigma\sigma^*$	basis set	Cl−O (Å)	Cl charge	ρ_{Cl}	ρ_O	$\sigma\sigma^*$
					(A) Hydroxyl−Cl^-						
$Cl-\dot{O}H^-$	2.07	−0.71	0.28	0.74	yes[b]	6-31G*	2.67	−0.95	0.0	1.0	no[c]
						6-31+G*	2.48	−0.81	0.11	0.94	sl[c]
$Cl-\dot{O}H(H_2O)^-$	2.05	−0.66	0.30	0.71	yes[b]	6-31G*	2.34	−0.85	0.14	0.91	yes[c]
						6-31+G*	2.23	−0.81	0.27	0.78	yes[c]
$Cl-\dot{O}H(H_2O)_6^-$	2.19	−0.63	0.14	0.89	yes[b]						
					(B) Water−$Cl^{\bullet}$						
$H_2O-Cl^{\bullet}$	2.03	−0.21	0.73	0.25	yes[d]	6-31G*	2.63	−0.04	0.97	0.04	v sl[d]
						6-31+G*	2.70	−0.02	0.98	0.02	v sl[d]
$H_2O-\dot{C}l(H_2O)_2$	2.02	−0.31	0.63	0.37	yes[d]	6-31G*	2.32	−0.15	0.85	0.18	yes[d]
						DN**	2.34	−0.26	0.59	0.42	yes[d,e]
$H_2O-\dot{C}l(H_2O)_5$	2.01	−0.35	0.57	0.43	yes[d]	6-31G*	2.29	−0.36	0.63	0.41	yes[f]

[a] The geometries obtained at the UMP2/6-31G* and UMP2/6-31+G* levels. Spin and charge densities are from the Mulliken population analyses of the SCF wave function only. [b] This was found to be a local minimum. In the globally optimized structure the OH hydrogen points toward the Cl^- and is lower in energy. Furthermore, in the optimized structure the full spin is found on OH without any $\sigma\sigma^*$ bonding (see text). [c] The ClOH angle was fixed at 96.3° (other comments in footnote *b* apply; see Figure 3 and text). [d] Full optimization at level indicated. [e] Density functional theory full optimization for $H_2O-\dot{C}l(H_2O)_2$ at the LSDA/VWN level. [f] This calculation started from the PM3 optimized structure and optimized only the coordinates of the $\sigma\sigma^*$ bonding water at the UMP2/6-31G* level.

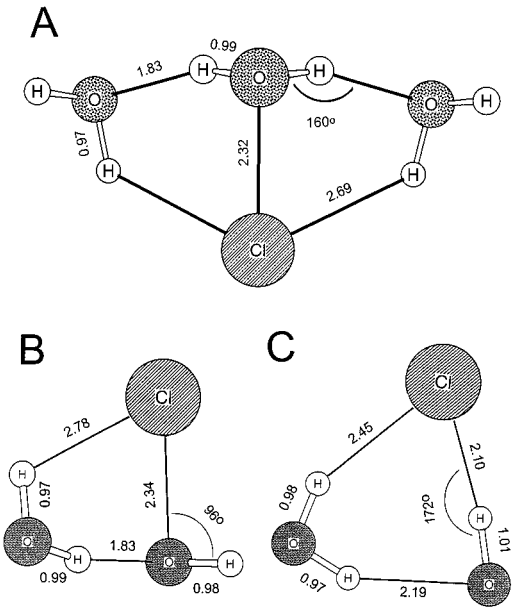

Figure 3. Ab initio UMP2/6-31G* structures of (A) fully optimized structure for $H_2O-\dot{C}l(H_2O)_2$, (B) structure of $Cl-\dot{O}H(H_2O)^-$, which is optimized with the ClOH angle fixed at 96.3° to allow for coupling of the OH radical center with the chloride ion, and (C) the fully optimized structure $Cl^-HO^{\bullet}(H_2O)$ in which the dipolar interaction dominates.

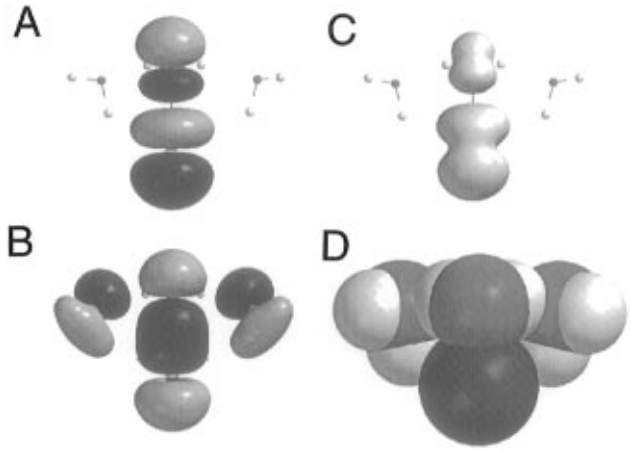

Figure 4. Space-filling model and orbital diagrams for the UMP2/6-31G* optimized structure of $H_2O-\dot{C}l(H_2O)_2$: (A) the σ^* orbital or HOMO from the UHF 6-31G* wave function, where this orbital contains the unpaired electron; (B) the σ bonding orbital (HOMO-6); (C) the spatial unpaired spin distribution (note that it compares well to the HOMO); (D) space-filling molecular model (chlorine = black, oxygen = gray, hydrogen = white).

hydrogen (−.043) suggests a coupling of ca. −22 G, which is not experimentally observed in our work but closely agrees with that found for $Cl-\dot{O}H^-$ in $SrCl_2$.[12] As mentioned, full optimization of $Cl-\dot{O}H(H_2O)^-$ at the ab initio level results in the rotation of the $OH^{\bullet}$ so that the hydroxyl hydrogen points toward the chloride ion: $Cl^-\cdots H-O^{\bullet}(H_2O)$ (Figure 3C), i.e, the optimized structure for $Cl^-\cdots H-O^{\bullet}(H_2O)$ at UMP2/6-31G* in Figure 3C found to be substantially more stable (ca. 16 kcal) than the structure shown in Figure 3B. For UMP2/6-31+G* structures the energy difference is again substantial, 11 kcal. No significant spin transfer occurs to Cl for the structure in Figure 3C, so it does not correspond to the experimental observations. At the PM3 level fixing of the ClOH bond angle is unnecessary, since geometry optimization finds a local minimum (at 96.3°), which suggests $\sigma\sigma^*$ bonding in both cases whose spin density distribution generally agrees with the results of the 6-31+G*(MP2) calculations. On further hydration of $Cl-\dot{O}H^-$ up to six waters, i.e., $Cl-\dot{O}H(H_2O)_6^-$, the PM3 calculation shows substantially decreased bond strength (as suggested by the predicted bond distance) and diminished spin transfer to chlorine. From these results we find no strong evidence that group A type structures can explain our experimental results, since the experimental results show no resolved hydrogen couplings and chlorine couplings that indicate about 60% spin on the chlorine atom not the maximum of 30% found for these calculations.

For Group B the ab initio calculations suggest little bonding of one H_2O and $Cl^{\bullet}$. In this case the 6-31+G*/UMP2 full optimization does not result in any significant change from the 6-31G*/UMP2. This is not unexpected, since in Group B only neutral species are considered. Full optimization at 6-31G*/UMP2 of the system of a $Cl^{\bullet}$ atom with three waters, $H_2O^{\bullet}Cl(H_2O)_2$,results in a significant shortening of the Cl−O distance to 2.32 Å (Figure 3A) in a clear coupling of the p orbitals on the chlorine and oxygen indicative of $\sigma\sigma^*$ bonding (Figure 4) and 18% of the total spin transferred from chlorine to the bonded water. In Figure 4 we show the σ^* MO (HOMO), σ MO (HOMO-6), the spatial spin distribution, and the space-filling

molecular model of the geometry-optimized trihydrated chlorine atom. The HOMO that contains the unpaired spin is found to be composed of a $3p_z$ orbital of chlorine and a $2p_z$ orbital of oxygen. The spin localization to the bonding orbitals is a defining characteristic of $\sigma\sigma^*$ bonding. Although the spin distribution follows the HOMO, as expected, spin polarization of inner shells contributes to the spin density at the positions of the nodal planes in the HOMO (Figure 4C). An additional calculation that fully optimized the $H_2O-\dot{C}l(H_2O)_2$ structure using the Spartan density functional theory code with a DN** basis set gave results also suggesting $\sigma\sigma^*$ bonding with substantially increased spin transfer from Cl to oxygen (see Table 2). The Cl spin density for this calculation is in good agreement with the experimental value (0.6). We note, however, that this type of calculation has a tendency to overestimate bonding.

Results found on increasing the hydration level to six waters are also given in Table 2. The fully optimized PM3 structure shows an increased spin transfer to the oxygen in the bonded water and a slight increase in bond strength (as evidenced by the bond length). Starting with this fully optimized PM3 structure, the coordinates of only the bonding water were optimized at the UMP2/6-31G* level. We find an increased bond strength and spin delocalization onto the bonding water oxygen as well as more charge transfer to chlorine over that found for the UMP2/6-31G* optimized structure for $H_2O-\dot{C}l-(H_2O)_2$ (Table 2). The calculated spin density on chlorine is in good agreement with the 0.6 value estimate from experiment. Furthermore, the calculated s orbital spin densities on the two hydrogens of the bonding water are −0.0185 and −0.0170, which correspond to about −9 G couplings. These couplings are within experimental line widths and are in keeping with the lack of experimental observation of additional hyperfine structure. The PM3 calculations are in good agreement with the ab initio results for the water−chlorine atom $\sigma\sigma^*$ interaction (Table 2) but tend to suggest stronger bonding than the ab initio calculations. Bonding is predicted even without waters of hydration. The spin transfer to water is also somewhat increased at the PM3 level but with actually smaller predicted hydrogen couplings of ca. −2 G. The PM3 predicted spin densities on Cl in each of the multiply hydrated structures $H_2O-\dot{C}l(H_2O)_n$ for $n = 3$ and 5 are also in good agreement with experimental results.

A consideration of the energetics of the chlorine atom−water interaction is of interest. We have performed several calculations on the overall reaction energetics for reaction 6.

$$Cl^{\bullet} + (H_2O)_3 \rightarrow {}^{\bullet}Cl(H_2O)_3 \qquad (6)$$

The change in PM3 heats of formation was −14.8 kcal, and the UMP2/6-31G* energy change for the reaction was −13.9 kcal. Energies for $Cl^{\bullet}$ and $(H_2O)_3$ were calculated separately with the geometry of the waters kept at the optimized ab initio (or PM3) geometry of the ${}^{\bullet}Cl(H_2O)_3$ system so that the energy change (or change in heats of formation) reflects the water−chlorine interaction only. No correction was made for basis set superposition error for the ab initio result, but corrections for similar systems amount to 2−3 kcal weakening of the water interaction energy.[29] A similar PM3 calculation for ${}^{\bullet}Cl(H_2O)_6$ gave −21 kcal for the chlorine atom interaction enthalpy with six waters. Solvent effects would be expected to affect these values. Futhermore, for systems with multiple waters the chlorine interaction has contributions from dipole and polarization interactions in addition to that contributed by $\sigma\sigma^*$ bonding.

Conclusions

Our experimental ESR results clearly show evidence for chlorine atom−water interaction at low temperatures. The chlorine atom spin density derived from the experimental chlorine hyperfine splitting (60%) suggests extensive delocalization onto the water species. Previous experimental work in aqueous solution[1−4] suggested the existence of $Cl-\dot{H}_2O$ and $Cl-\dot{O}H^-$ adducts as intermediates in Cl atom chemistry, and our experimental and theoretical results give strong evidence for the existence of one of these species.

Although the specific nature of the water component is not known from our experimental results, ab initio and semiempirical molecular orbital calculations shed some light on these likely intermediates. Neither $Cl-\dot{H}_2O$ or $Cl-\dot{O}H^-$ is found to show significant $\sigma\sigma^*$ bonding without additional waters of hydration in ab initio calculations that include correlation corrections at the MP2 level. Only on addition of waters of hydration do calculations predict bonding interactions in both systems. Best agreement with the experimental hyperfine couplings and the implied spin density distribution is found in both ab initio and semiempirical calculations for the chlorine atom−water interaction model, $H_2O-\dot{C}l(H_2O)_n$. As the number of water molecules increases, the Cl−O distance decreases and delocalization onto oxygen increases.

The predicted hyperfine couplings of the OH hydrogen in $Cl-\dot{O}H(H_2O)^-$ (ca. 22 G) are not in agreement with the experimental lack of resolved hyperfine structure. The predicted small hydrogen couplings (9 G) for the bonding water hydrogens in $H_2O-\dot{C}l(H_2O)_5$ are in better accord with experimental results, which show no hyperfine structure beyond that found for chlorine. For the $Cl^-\dot{O}H(H_2O)$ system a $\sigma\sigma^*$ interaction only occurs at a fixed Cl−O−H bond angle, and the lowest energy ab initio structure for this system actually favors the structure in Figure 3C with the OH hydrogen pointing toward chlorine, i.e., $Cl^-\cdots HO^{\bullet}(H_2O)$, which is dominated by ion−dipole interactions, not $\sigma\sigma^*$ bonding. Yu et al. found similar results for the $NH_3-H_2O^{\bullet+}$ interaction where the hydrogen-bonded species ($H_2O\cdots HNH_2^{\bullet+}$) was 17 kcal lower in energy than the $\sigma\sigma^*$ species ($H_2O-\dot{N}H_3^+$).[30] For the $Cl^-\dot{O}H(H_2O)$ system in a frozen fully solvated system many orientations are likely and we cannot completely discount the possibility of an $OH^{\bullet}-Cl^-$ $\sigma\sigma^*$ interaction. However, the following facts argue that it is the $H_2O-\dot{C}l(H_2O)_n$ system that we are observing experimentally. (1) MO calculations show that the lowest energy structure of $H_2O-\dot{C}l(H_2O)_n$ is the $\sigma\sigma^*$ bonded structure, whereas geometry constraints are necessary for $Cl-\dot{O}H(H_2O)^-$. (2) All levels of theory for $H_2O-\dot{C}l(H_2O)_n$ predict $\sigma^2\sigma^{*1}$ bonding. (3) The Cl atom spin density in this structure ($n = 5$) is predicted to be close to the experimental value. No such agreement was found for $Cl-\dot{O}H(H_2O)_6^-$. (4) Small proton hyperfine couplings are predicted for $H_2O-\dot{C}l(H_2O)_n$, in agreement with the lack of observation of experimental proton hyperfine couplings; however, observable hydrogen couplings were predicted for $Cl-\dot{O}H(H_2O)^-$. (5) Calculations that increase the number of hydrating waters increase the strength of the interaction in $H_2O-\dot{C}l(H_2O)_n$ and weaken it in the case of $Cl-\dot{O}H(H_2O)_n^-$. We conclude that the structure, $H_2O-\dot{C}l(H_2O)_n$, best accounts for our experimental observations. Our results also clearly suggest that that the energy of the SOMO of the aquated chlorine atom is appropriate for bonding to the HOMO of the water molecule as depicted in Figure 5.

We note that the $\sigma\sigma^*$ bonding indicated in our results for $H_2O-\dot{C}l(H_2O)_n$ would reduce the reactivity and increase the selectivity of chlorine atoms relative to their behavior in inert media. At this point we cannot resolve the interesting contro-

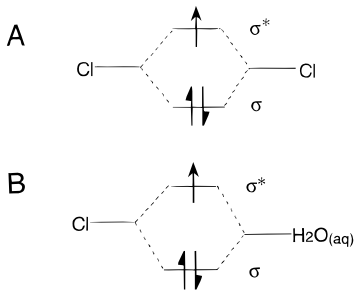

Figure 5. Interaction diagrams for chlorine atom and water species. (A) Many species such as $^{\bullet}Cl_2^-$ are well-known to form $\sigma^2\sigma^{*1}$ three-electron bonds as shown (see Table 1). (B) In aqueous solutions our experimental and theoretical results suggest that the chlorine atom forms a $\sigma^2\sigma^{*1}$ three-electron bond with water, resulting in $Cl-\dot{O}H_{2(aq)}$.

versy as to the whether there should be an absorption at 320 nm for this species;[3−5] but similar species do have absorptions in this range.[13] Finally, it is interesting to note that the bonding between chlorine atoms and water may extend to the atmospheric chemistry of chlorine atoms.

Acknowledgment. We thank the National Cancer Institute of the National Institutes of Health (Grant RO1CA45424), the Office of Health and Environmental Research of the Department of Energy (Grant DEFG028ER60455), and the Oakland University Research Excellence Program in Biotechnology for support of this work.

Supporting Information Available: Computer outputs of *x*, *y*, *z* coordinates for ab initio optimized $^{\bullet}Cl(H_2O)_n$ and $^{\bullet}ClOHH_2O^-$species (7 pages). Ordering information is given on any current masthead page.

References and Notes

(1) Nagarajan, V.; Fessenden R. W. *J. Phys. Chem.* **1985**, *89*, 2330.
(2) Jayson, G. G.; Parsons, B. J.; Swallow, A. J. *J. Chem. Soc., Faraday Trans. 1* **1973**, *69*, 1597.
(3) Treinin, A.; Hayon, E. *Int. J. Radiat. Phys. Chem.* **1975**, *7*, 387.
(4) Treinin, A.; Hayon, E. *J. Am. Chem. Soc.* **1975**, *97*, 1716.
(5) Adams, J.; Barlow, S.; Buxton, G. V.; Malone, T. M.; Salmon, G. A. *J. Chem. Soc., Faraday Trans. 1* **1995**, *91*, 3303.
(6) Schulz, P. A.; Mead, R. D.; Jones, P. L.; Lineberger, W. C. *J. Chem. Phys.* **1982**, *77*, 1153.
(7) Trainham, R.; Fletcher, G. D.; Larson, D. J. *J. Phys. B: At. Mol. Phys*. **1987**, *20*, L777.
(8) Abu-Raqabah, A.; Symons, M. C. R. *J. Chem. Soc., Faraday Trans.* **1990**, *86*, 3293.
(9) Abu-Raqabah, A.; Symons, M. C. R. *J. Am. Chem. Soc.* **1990**, *112*, 8614.
(10) Raynor, J. B.: Rowland, I. J.; Symons, M. C. R. *J. Chem. Soc., Faraday Trans.* **1991**, *87*, 571.
(11) Pace, D.; Ezell, K.; Kispert, L. D. *J. Chem Phys.* **1979**, *71*, 3971.
(12) Catton, R. C.; Symons, M. C. R. *J. Chem. Soc. A* **1969**, 446.
(13) Champagne, M.; Mullins, M.; Colson, A.-O.; Sevilla, M. D. *J. Phys. Chem.* **1991**, *95*, 6487.
(14) Brivati, J. S.; Symons, M. C. R.; Tinling, D. J. A.; Wardale, H. W.; Williams, D. O. *Chem. Commun.* **1965**, 402.
(15) Claxton, T. A.; Ginns, I. S.; Godfrey, M. J.; Rao, K. V. S.; Symons, M. C. R. *J. Chem. Soc., Faraday Trans.* **1973**, *69*, 217.
(16) Lias, S. G.; Bartness, J. E.; Liebman, J. F.; Holmes, J. L.; Levin R.; Mallard, W. G. *J. Phys. Chem. Ref. Data, Suppl. 1* **1988**, *17*.
(17) Frisch M. J.; Trucks, G. W.; Head-Gordon, M.; Gill, P. M. W.; Wong, M. W.; Foresman, J. B.; Johnson, B. G.; Schlegel, H. B.; Robb, M. A.; Replogle, E. S.; Gomperts, R.; Andres, J. L.; Raghavachari, K.; Binkley J. S.; Gonzalez, C.; Martin, R. L.; Fox, D. J.; Defrees, D. J.; Baker, J.; Stewart, J. J. P.; Pople, J. A. *GAUSSIAN 92*, Revision C; Gaussian, Inc.: Pittsburgh, PA, 1992.
(18) Stewart, J. J. P. *J. Comput. Chem*. **1989**, *10*, 210.
(19) Hariharan, P. C.; Pople, J. A. *Chem. Phys. Lett.* **1972**, *66*, 217.
(20) Roothaan, C. C. J. *Rev. Mod. Phys.* **1960**, *32*, 179.
(21) Binkley, J. S.; Pople, J. A.; Dobosh, P. A. *Mol. Phys.* **1974**, *28*, 1423.
(22) Pople, J. A.; Nesbet, R. K. *J. Chem. Phys.* **1954**, *22*, 571.
(23) Moller, C.; Plesset, M. S. *Phys. Rev.* **1934**, *46*, 618.
(24) Kohn, W.; Sham, L. *J. Phys. Rev. A* **1965**, *140*, 1133.
(25) Slater, J. C. *Quantum Theory of Molecular and Solids*. McGraw-Hill: New York, 1974; Vol. 4.
(26) Vosko, S. H.; Wilk, L.; Nusair, M. *Can. J. Phys*. **1980**, *58*, 1200.
(27) Schlegel, H. B. *J. Comput. Chem*. **1982**, *3*, 214.
(28) (a) Mulliken, R. S. *J. Chem. Phys*. **1955,** *23*, 1833. (b) Szabo, A.; Ostlund, N. S. In *Modern Quantum Chemistry*; McGraw-Hill: New York, 1989.
(29) Colson, A.-O.; Sevilla, M. D. *J. Phys. Chem*. **1994**, *98*, 10484.
(30) Yu, D.; Rauk, A.; Armstrong, D. A. *Can. J. Chem*. **1994**, *72*, 471.